ISSN 1070-3632, Russian Journal of General Chemistry, 2014, Vol. 84, No. 7, pp. 1417–1428. © Pleiades Publishing, Ltd., 2014.

Infrared, Raman, ^{1}H NMR, TG, and SEM Properties of the Charge-Transfer Interactions between Tris(hydroxymethyl)methane with the Acceptors Picric Acid, Chloranilic Acid, and 1,3-Dinitrobenzene[1]

Moamen S. Refat[a,b], Hosam A. Saad[a,c], and Abdel Majid A. Adam[a]

[a] *Department of Chemistry, Faculty of Science, Taif University, Al-Haweiah, P.O. Box 888, Zip Code 21974, Taif, Saudi Arabia*
e-mail: msrefat@yahoo.com

[b] *Department of Chemistry, Faculty of Science, Port Said University, Port Said, Egypt*

[c] *Department of Chemistry, Faculty of Science, Zagazig University, Zagazig, Egypt*

Received March 10, 2014

Abstract—Intermolecular charge-transfer complexes (CT) between the tris(hydroxymethyl)methane (THM) as a donor and picric acid (PA), chloranilic acid (CLA) and 1,3-dinitrobenzene (DNB) as a π-acceptor have been structurally, thermally and morphologically studied in methanol at room temperature. Based on elemental analyses (CHN), the stoichiometry of the obtained CT complexes (THM: acceptor molar ratios) was determined to be 1 : 1 for all three complexes. The CT complexes have been characterized via elemental analyses (CHN), IR, Raman and ^{1}H NMR spectroscopy in order to predict the position of the CT interaction between the donating and accepting sites. Thermal decomposition behavior of these complexes was also investigated, and their kinetic thermodynamic parameters were calculated with Coats-Redfern and Horowitz-Metzger methods. Finally, the microstructure properties of these complexes were observed using scanning electron microscope (SEM).

Keywords: tris(hydroxymethyl)methane, charge-transfer complex, thermal analysis, thermodynamic parameters

DOI: 10.1134/S1070363214070305

INTRODUCTION

Charge-transfer complex (CT) was first introduced by Mulliken [1, 2] and has been widely discussed by Foster [3]. Mulliken [4, 5] demonstrated that the CT interactions within a molecular complex that consists of an electron donor, D, and an electron acceptor, A, involve a resonance with a transfer of charge from D to A. CT complexation is of great importance in chemical reactions, including addition, substitution, condensation [6], biochemical and bioelectrochemical energy-transfer processes [7], biological systems [8], and drug–receptor binding mechanisms. For example, drug action, enzyme catalysis, ion transfers through lipophilic membranes [9], and certain π-acceptors have been successfully utilized in the pharmaceutical analysis of some drugs in pure form or in pharmaceutical preparations [10–12]. Furthermore, CT complexation is also of great importance in many applications and fields, such as in non-linear optical materials, electrically conductive materials, second-order non-linear optical activity, microemulsions, surface chemistry, photocatalysts, dendrimers, solar energy storage, organic semiconductors, and the investigation of redox processes [13–18]. CT complexes that use organic species are intensively studied because of their special type of interaction, which is accompanied by the transfer of an electron from the donor to the acceptor [19]. In addition, the protonation of the donor from acidic acceptors is a route for the formation of ion-pair adducts [20]. The purpose of the work reported here was to study the structural and thermal stability of CT complexes formed between tris(hydroxymethyl)methane (THM) as a donor with picric acid (PA), chloranilic acid (CLA), and 1,3-dinitrobenzene (DNB) as a π-acceptor. These complexes are

[1] The text was submitted by the authors in English.

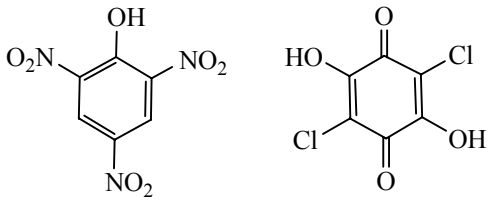

PA

CLA

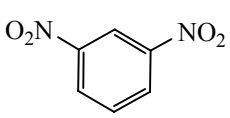

DNB

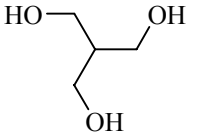

THM

Scheme 1. Structures of the THM donor and the acceptors.

readily prepared from the reaction of the THM donor with PA, CLA and DNB acceptors in methanol media. The synthesized CT complexes were structurally characterized to interpret the behavior of interactions using IR, Raman, ^{1}H NMR techniques and elemental analyses (CHN). The thermal behavior of the obtained complexes and the kinetic thermodynamic parameters (E^*, A, ΔS^*, ΔH^*, and ΔG^*) were also investigated. Finally, the structural morphology of the obtained complexes was established by scanning electron microscope (SEM).

EXPERIMENTAL

General procedure. All chemical used were of high grade. Tris(hydroxymethyl)methane (with a stated purity of greater than 99.8%) (THM; $C_4H_{10}O_3$; 106.12) and the picric acid (PA; $C_6H_3N_3O_7$; 229.10), chloranilic acid (CLA; $C_6H_2Cl_2O_4$; 208.98) or 1,3-dinitrobenzene (DNB; $C_6H_4N_2O_4$; 168.11) acceptors (Scheme 1) were obtained from Sigma-Aldrich Chemical Company, USA and were used without further purification. Commercially available spectroscopic grade methanol solvent was purchased from Merck Chemical Company and was also used as received. The elemental analyses of the carbon, hydrogen and nitrogen contents were determined with the Micro analyzer Perkin-Elmer CHN 2400 (USA) at Cairo University, Egypt. The infrared (IR) spectra were measured as KBr discs within the range of 4000–400 cm^{-1} on a Shimadzu FT-IR spectrophotometer (Japan) with 30 scans at 2 cm^{-1} resolution at Taif University, Saudi Arabia. ^{1}H NMR spectra were collected by the Analytical Center at King Abdul Aziz University, Saudi Arabia, on a Bruker DRX-250 spectrometer operating at 250.13 MHz with a dual 5 mm probe head. The measurements were performed at ambient temperature using DMSO-d_6 (dimethylsulfoxide, d_6) as a solvent and TMS (tetramethylsilane) as an internal reference. The ^{1}H NMR data are expressed in parts per million (ppm) and are internally referenced to the residual proton impurity in the DMSO solvent. The thermogravimetric analysis (TG) was carried under a static air atmosphere to a temperature of 800°C at a heating rate of 10°C/min using a Shimadzu TGA–50H thermal analyzer (Japan) in the Central Lab at the Ain Shams University, Egypt. Microstructure properties of the prepared CT complexes were observed using scanning electron microscope (SEM) (Jeol JSM-6390 instrument). The instrument was operated at an accelerating voltage of 20 kV.

Senthetic procedure. The solid THM complexes with the PA, CLA or DNB acceptor were prepared by mixing equimolar amounts of the THM donor with each acceptor in pure–grade methanol. The resulting solutions were stirred for approximately 30 min and allowed to evaporate slowly at room temperature. The separated solid complexes were filtered and washed well with methanol. Then, the CT complexes were collected and dried over anhydrous calcium chloride for 24 h in desiccator.

RESULTS AND DISCUSSION

Systematic IUPAC nomenclature. The systematic IUPAC names of the THM donor, acceptors and the formed CT complexes are:

– THM; 2-(hydroxymethyl)propane-1,3-diol [Tris-(hydroxymethyl)methane];

– PA; 2,4,6-trinitrophenol (Picric acid);

– CLA; 2,5-dichloro-3,6-dihydroxy-1,4-benzoquinone (Chloranilic acid);

– DNB; 1,3-dinitrobenzene;

– [(THM)(PA)] complex; 2,4,6-trinitrophenol-2-(hydroxymethyl)propane-1,3-diol;

– [(THM)(CLA)] complex; 2,5-dichloro-3,6-dihydroxybenzo-1,4-quinone-2-(hydroxymethyl)propane-1,3-diol;

– [(THM)(DNB)] complex; 2-(hydroxymethyl)-propane-1,3-diol-1,3 dinitrobenzene.

Elemental analyses results. Elemental analyses (C, H, and N) of the THM CT complexes were

Table 1. Infrared frequencies (cm^{-1}) and tentative assignments for THM donor, acceptors and their complexes

THM donor	Acceptor			Complexes			Assignments
	PA	CLA	DNB	THM-PA	THM-CLA	THM-DNB	
3332	3374	3235	–	3229	3462	3350	ν(O–H)
			–		3268	3193	
			3110		3022	3105	ν(C–H); aromatic
2969	2928	–	–	2988	2946	2942	ν_s(C–H) + ν_{as}(C–H)
2872	2861			2830		2873	
–	–	–	–	2748	2600	2782	Hydrogen bond
				2692	2559	2727	
				2598	2501	2688	
				2461			
–		1663	–	–	1680	–	ν(C=O), CLA, complex
		1629			1614		
–	1616		1608	1633	–	1597	ν_{as}(NO_2); PA, DNB, complex
–	1567		–	1559	1534	1536	Ring breathing bands
1464	1541		1538	1486	1490	1467	ν(C=C)
1407	1492			1437	1464	1399	δ(C–H) deformation
	1442				1389		
	1416						
1377	1357	1368	1364	1370	1350	1350	ν(C–C) + ν(C–O) + ν_{as}(C–N)
1301	1303	1263	1150	1334	1293	1216	
1268	1276	1207	1069	1270	1199	1155	
1225	1226	1168		1160	1066	1037	
1161	1180			1036	1045		
1038	1108						
	1078						
	1021						
964	888	981	914	906	988	908	δ(CH) in-plane bending
872	832	838	837	795	881	814	ν(C–Cl); CLA, complex
784	805	751	727	745	839	714	
	699			706	780	653	
				670			
–	626			626	–	630	δ(C–N) out-of-plane bending
	–	690		595	567		skeletal vibration
	543	569	663	547	–		δ(ONO); PA, DNB, complex
					434		CNC deformation.

performed, and the obtained analytical data are as follows:

(1) [(THM)(PA)]: $C_{10}H_{13}N_3O_{10}$; M_w = 335.22; orange. Calculated, %: C 35.83; H 3.91; N 12.53. Found, %: C 35.79; H 3.97; N 12.48.

(2) [(THM)(CLA)]; $C_{10}H_{12}Cl_2O_7$; M_w = 315.10; dark red. Calculated, %: C 38.12; H 3.84. Found, %: C 38.00; H 3.88.

(3) [(THM)(DNB)]; $C_{10}H_{14}N_2O_7$; M_w = 274.23; brown. Calculated, %: C 43.80; H 5.15; N 10.22. Found, %: C 43.85; H 5.09; N 10.27

It can see that the resulting values are in good agreement with the calculated values, and the suggested values are in agreement with the results obtained from the thermal decomposition. The stoichiometry of all complexes was found to be 1 : 1 ratios. Based on the obtained data, the formed CT complexes

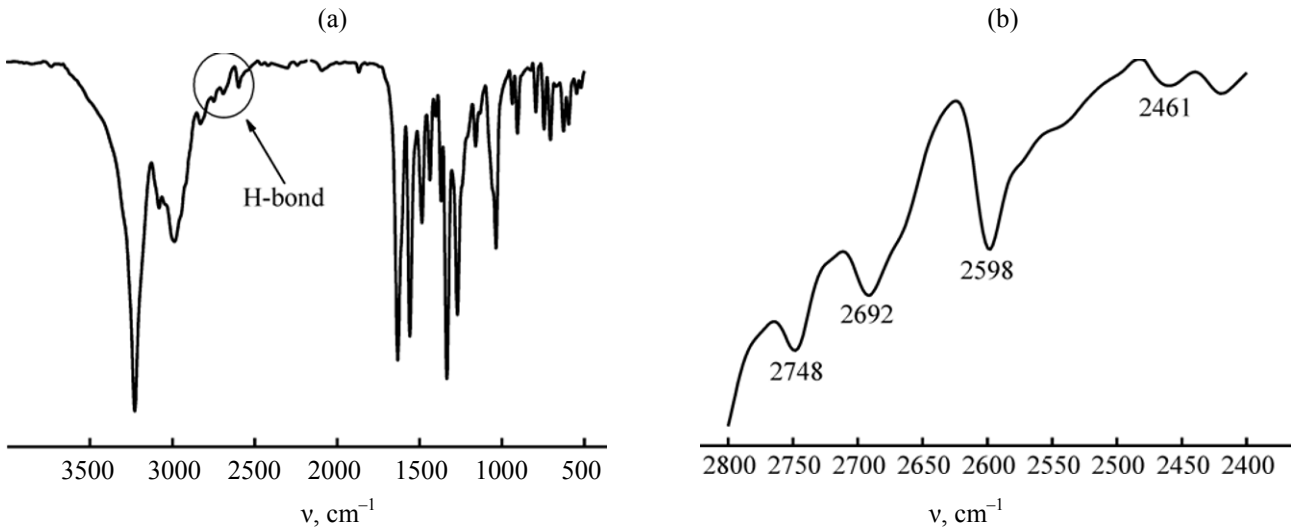

Fig. 1. (a) IR spectrum of THM-PA complex and (b) IR bands of THM-PA complex, which may assign to intermolecular H-bond.

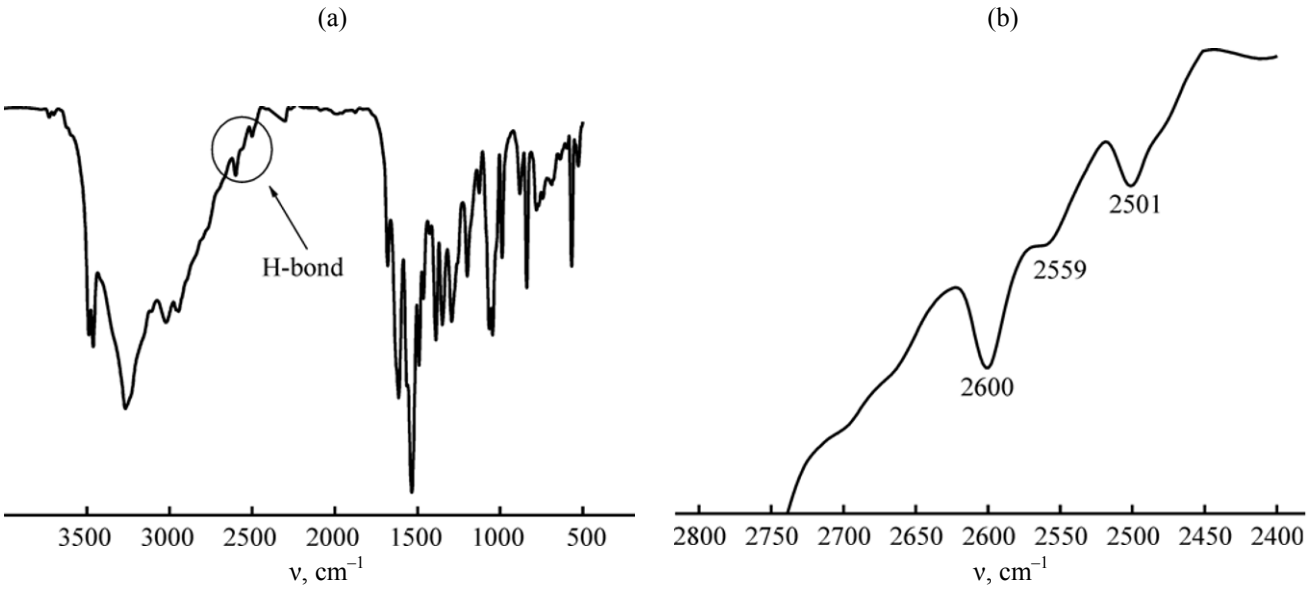

Fig. 2. (a) IR spectrum of THM-CLA complex and (b) IR bands of THM-CLA complex, which may assign to intermolecular H-bond.

were formulated as [(THM)(PA)], [(THM)(CLA)], and [(THM)(DNB)]. All the complexes are insoluble in cold and hot water, but easily soluble in DMF and DMSO solvents. The formation of 1 : 1 complexes was strongly supported by IR, ^{1}H NMR and thermal analyses. The PA, CLA and DNB complexes have a yellow, dark red and brown color, respectively.

Vibrational spectra. The IR absorption spectra of the THM solid CT complexes which registered in the frequency range 4000–400 cm^{-1} using KBr disc are shown in Figs. 1–3, and their characteristic IR band assignments for these complexes are provided in Table 1. The formation of the CT complexes is strongly supported by observing of main infrared bands of the THM donor and acceptors in the products spectra. However, the bands of the donor and acceptors in the complexes spectra reveal small shift in frequency and changes in their band intensities compared with those of the free donor and acceptors. This situation could be interpreted based on the expected changes in symmetry and electronic structure changes upon the formation of the CT complexes.

The spectrum of free THM donor displays a strong broad band at 3332 cm^{-1}, which may assign to

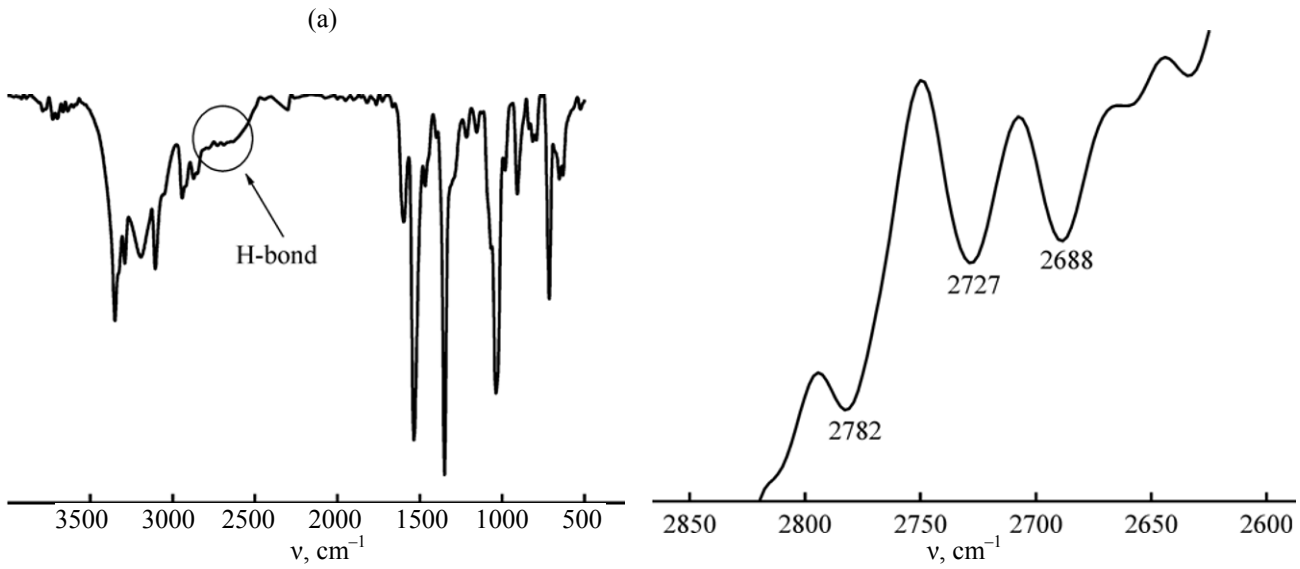

Fig. 3. (a) IR spectrum of THM-DNB complex and (b) IR bands of THM-DNB complex, which may assign to intermolecular H-bond.

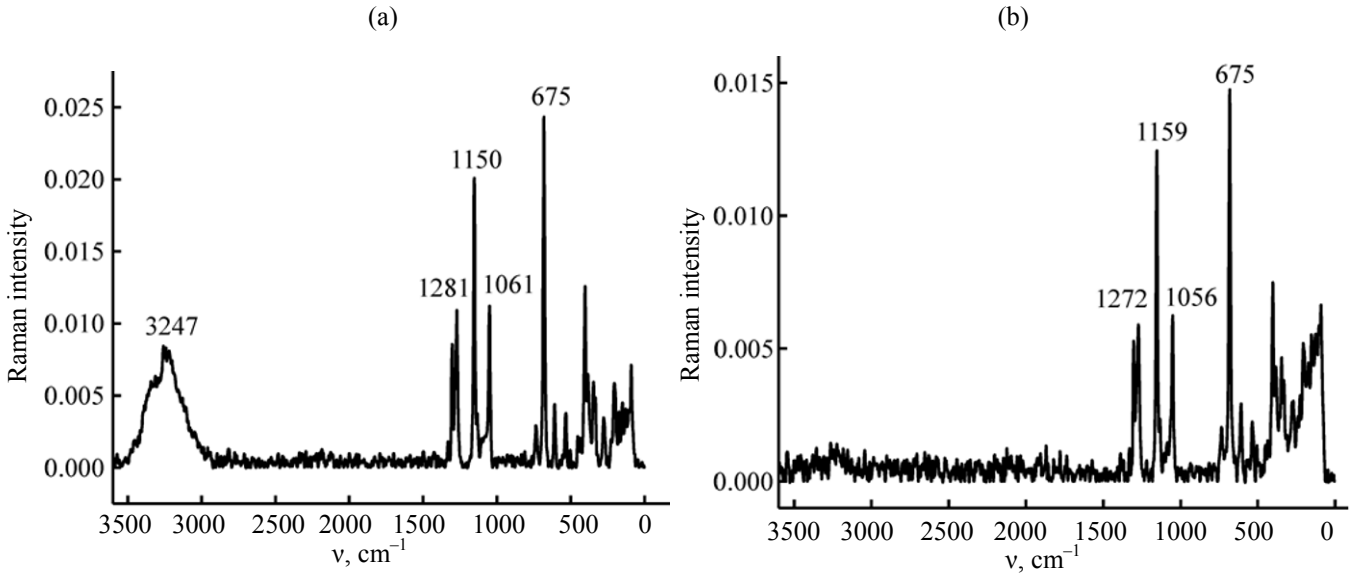

Fig. 4. Raman spectrum of (a) THM-PA complex and (b) THM-DNB complex.

ν(O–H) stretching vibration. In the IR spectra of the CT complexes, this characteristic band is shifted and decreased in intensity. The outlined changes in ν(O–H) in the THM donor upon complexation clearly confirm the involvement of one oxygen atom of the O–H group in hydrogen bonding with acceptors. This bonding is confirmed by the appearance of a weak absorption bands that appear between 2400–2800 cm^{-1}, representing the H-bonded OH group. These group of bands were observed at 2748, 2692, 2598, and 2461 cm^{-1} for PA complex (Fig. 1b), at 2600, 2559, and 2501 cm^{-1} for CLA complex (Fig. 2b), and at 2782, 2727 and 2688 cm^{-1} for DNB complex (Fig. 3b). These bands are due to hydrogen bonding in the complex which clearly indicates that the complexation occurs through the formation of intermolecular H-bond between the O–H group in the THM donor and acceptors [21–25]. Furthermore, in CLA complex, the carbonyl stretching vibration bands; ν(C=O) appeared at 1680 and 1614 cm^{-1}, slightly shifted with respect to those of CLA (1663 and 1629 cm^{-1}); this is probably due to intermolecular H-bond with THM. Concerning

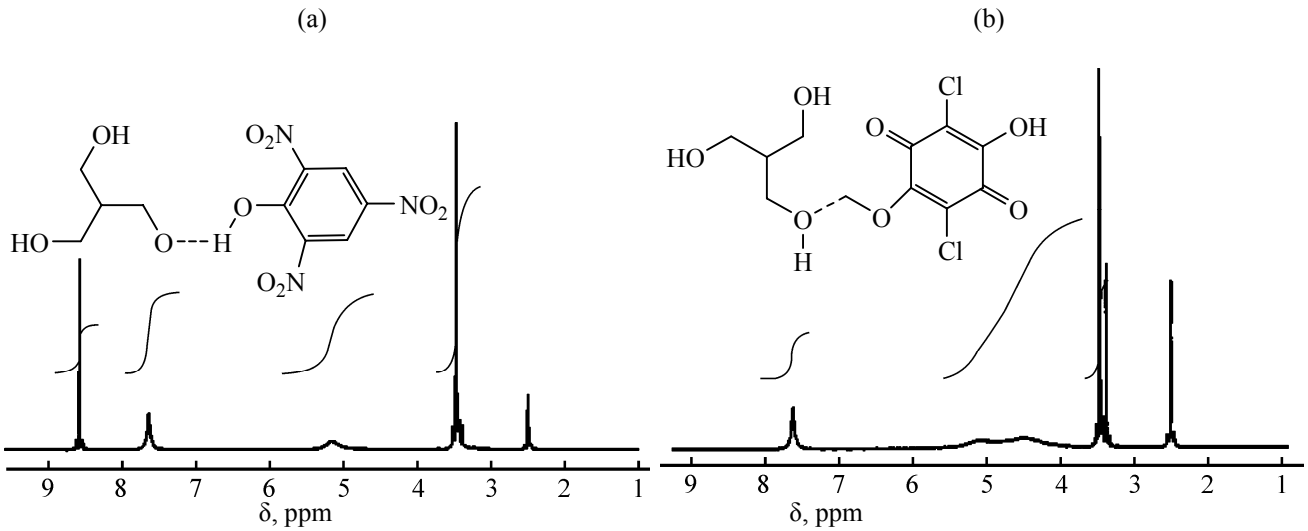

Fig. 5. (a) ^{1}H NMR spectrum of (a) THM-PA complex and (b) THM-CLA complex.

ν(C–Cl) vibrational bands, they are recorded at 839 and 780 cm^{-1} in the complex spectrum compared with 838 and 751 cm^{-1} for CLA alone.

The electron density around protons depends on the degree of electro negativity for atoms attached with protons; therefore, the two withdrawing nitro groups attached to DNB acceptor decrease the electron density around the proton flanked between the nitro groups, and increase the acidic character of this proton which facilitates to make intermolecular hydrogen bond with the lone pair of electron on the oxygen atom of the THM donor [26, 27].

Figure 4 shows the representative laser Raman spectra of the [(THM)(PA)] and [(THM)(DNB)] complexes. The Raman spectra for the PA and DNB complexes exhibited a very intense band at 1150–675 and 1159–675 cm^{-1}, respectively, which clearly correspond to symmetric vibrational modes of ν(C–C) and bending deformation of δ(C–N), respectively. The symmetric vibrational modes of ν(C–N) for the PA and DNB complexes appear at 1281 and 1272 cm^{-1}, respectively. The Raman band of ν(O–H) hydroxyl group was observed as a broad band at 3247 cm^{-1} in the spectrum of the PA complex.

^{1}H NMR spectra. The H-bonded complexes between THM with PA and CLA acceptors was further confirmed by measuring the ^{1}H NMR spectrum of the formed complex. The 400 MHz nuclear magnetic resonance (^{1}H NMR) spectrum of the [(THM)(PA)] complex was measured in DMSO-d_6 at room temperature and is given in Fig. 5a. The reaction of THM with PA yielded a new CT complex, which produced signals at δ = 3.38 m (1H, CH), 3.47 d (6H, 3CH_2), 5.10 b (1H, $CH_2O\underline{H}$ hydrogen atom bonded to oxygen atom which forms hydrogen bond), 5.15 b (2H, 2$CH_2O\underline{H}$), 7.64 s (1H, hydrogen bonded OH of picric acid), 8.58 s (2H, picric acid protons). The new broad peak observed at 5.10 ppm in this complex, is attributed to the formation of a hydrogen bond between PA and THM. The peak at δ = 11.94 ppm, which is assigned to the (–OH) proton of free picric acid [28], was up-field shift to 7.64 ppm in the spectrum of this complex. Together, these data indicate that the hydroxyl and phenolic groups are involved in the formation of the CT complex between THM and PA.

The [(THM)(CLA)] complex produced signals (Fig. 5b) at δ = 3.33 m (1H, CH), 3.47 d (6H, 3CH_2), 4.54 b (1H, $CH_2O\underline{H}$ hydrogen atom bonded to oxygen atom which forms hydrogen bond), 5.10 b (3H, 2$CH_2O\underline{H}$ and chloranilic acid OH), 7.65 s (1H, hydrogen bonded OH of chloranilic acid). It has been found that, the phenolic proton (–OH) signal, which is observed at approximately δ ~ 9.15 ppm in the spectrum of the free CLA acceptor [29] , decreased in intensity with a high up-field shift for the non-hydrogen-bonded one (δ ~ 4.54) in the spectrum of this complex. Instead, the peak appeared at 7.65 ppm, is attributed to the hydrogen bonded OH of CLA. This situation confirmed the formation of the CT complex between one of the phenolic protons of CLA to one of the –OH groups of THM. The two signals at 3.33 ppm

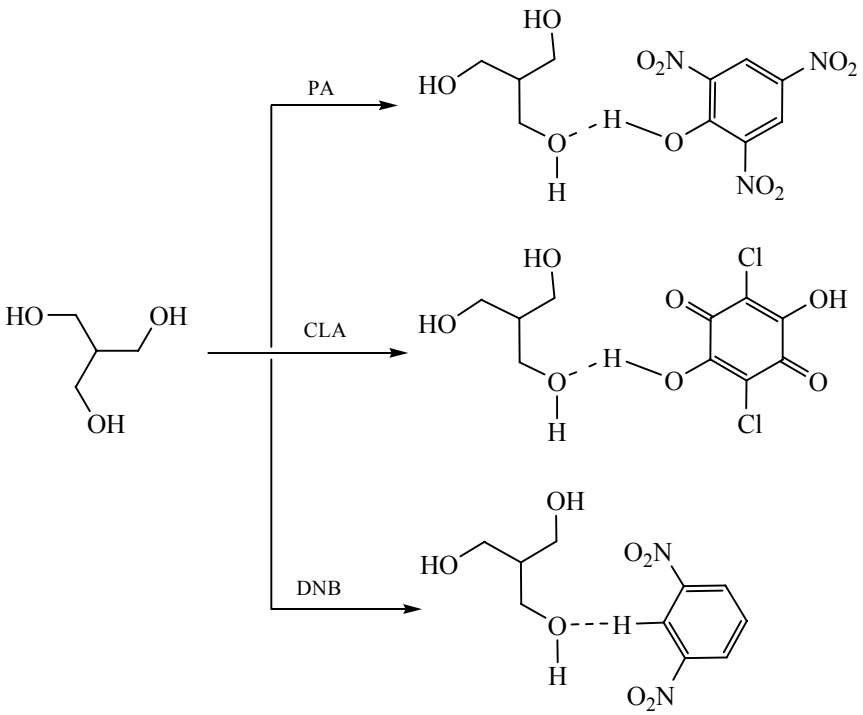

Scheme 2. Proposed complexation mechanism between THM donor and acceptors.

(1H) and 3.47 ppm (6H), corresponding to the protons of CH and CH_2 groups, respectively. Based on the results obtained, the suggested complexation mechanism between THM donor with acceptors is illustrated in Scheme 2.

Thermal degradation results. To confirm the composition and structures of the formed solid CT complexes, thermogravimetric analysis (TG) was carried out for these complexes over a temperature range of 25–800°C under a static air atmosphere. Their representative thermograms are illustrated in Fig. 6, whereas the possible thermal analysis data for these complexes are provided in Table 2. The obtained data strongly support the structures proposed for the new synthesized complexes. The TG thermogram of the [(THM)(PA)] complex indicated that this complex was thermally decomposed in two degradation steps. The first decomposition step in the temperature range of 200–260°C has a weight loss of approximately 67.89% and is attributed to the loss of the acceptor moiety (PA). The final decomposition step occurred within the

Table 2. Thermal decomposition data for the THM CT complexes

Complex	Stages	TG range (°C)	TG% mass loss		Lost species
			found	calculated	
[(THM)(PA)]	I	200–260	67.89	68.34	PA acceptor
	II	260–800	31.62	31.66	THM donor
[(THM)(CLA)]	I	120–290	33.70	33.68	THM donor
	II	290–700	65.91	66.32	CLA acceptor
[(THM)(DNB)]	I	100–500	99.88	100.0	THM + DNB

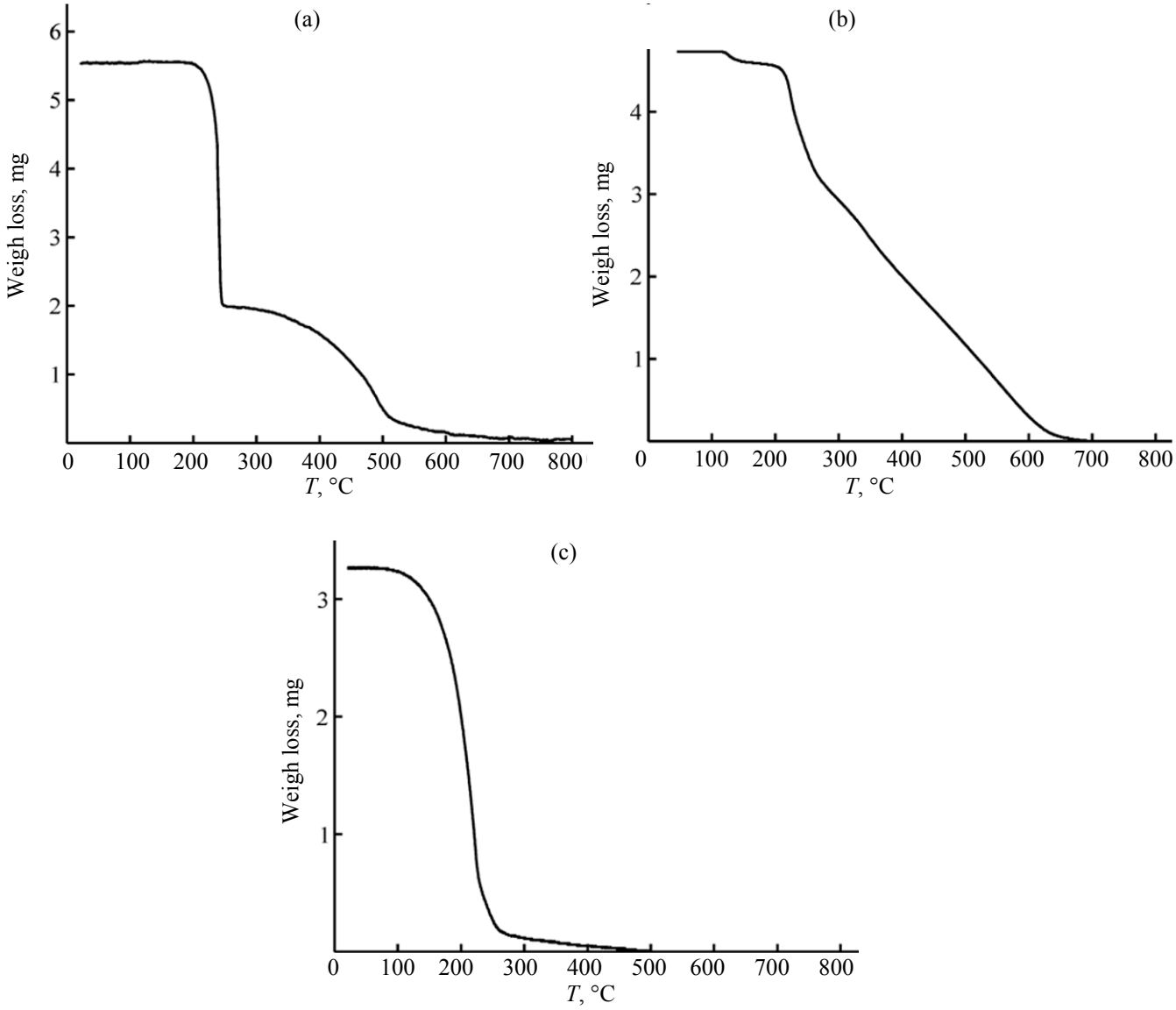

Fig. 6. TG thermogram of THM CT complexes: (a) THM-PA complex, (b) THM-CLA complex, and (c) THM-DNB complex.

260–800°C temperature range and was assigned to the removal of the donor moiety (THM). The thermal degradation of the [(THM)(CLA)] complex occurs in two degradation stages within the 120–700°C temperature range. The first stage of decomposition corresponds to the loss of the donor moiety with a weight loss of 33.70% very close to the expected theoretical value of 33.68%. The second stage of decomposition corresponds to the loss of the CLA moiety with a weight loss of 65.91%, which is in good agreement with the calculated value (66.32%). The TG thermogram of the DNB complex indicated that it is thermally stable in the 25–100°C temperature range. The thermal decomposition of this complex proceeds via one degradation step. The decomposition begins at ~100°C and was complete at ~500°C, and the observed weight loss associated with this step is (observed = 99.88, calculated = 100.0%), which can be attributed to the loss of the $C_{10}H_{14}N_2O_7$ moiety (THM+DNB).

Kinetic thermodynamic results. Recently, there has been increasing interest in determining the rate-dependent parameters of solid-state non-isothermal decomposition reactions by analysis of the TG curves. Several equations have been proposed to analyze a TG curve and to obtain the kinetic parameters. Two different methods were employed to evaluate the kinetic thermodynamic parameters: the Coats–Redfern

Table 3. Kinetic parameters determined using the Coats-Redfern (CR) and Horowitz-Metzger (HM) methods

Complex	Method	Parameter					r
		E, kJ/mol	A, s^{-1}	ΔS, J mol^{-1} K^{-1}	ΔH, kJ/mol	ΔG, J/mol	
[(THM)(PA)]	CR	37.0	4.00E+02	–195	35.0	105	0.9730
	HM	37.2	1.75E+03	–185	34.2	103	0.9714
[(THM)(DNB)]	CR	71.5	2.00E+04	–165	67.0	164	0.9999
	HM	88.4	2.50E+06	–130	89.0	163	0.9982
[(THM)(CLA)]	CR	185.0	1.21E+10	–61	178.0	230	0.9960
	HM	191.0	4.63E+10	–49	182.0	225	0.9941

method [30] and the Horowitz–Metzger method [31]. The thermodynamic parameters [i.e., the activation energy (E^*), the frequency factor (A), the enthalpy of activation (H^*), the entropy of activation (S^*), and the Gibbs free energy of activation (G^*)] associated with the complexes were evaluated graphically (Fig. 7) by employing the Coats-Redfern and Horowitz-Metzger methods, and the evaluated data are listed in Table 3. The kinetic data obtained from the two methods are comparable and can be considered in good agreement with each other. The activation energy (E^*) of the complexes is expected to increase with the increasing thermal stability of complexes. Therefore, the E^* value for the CLA complex is higher compared to the PA and DNB complexes, which indicates the higher thermal stability of the CLA complex. The negative values of the ΔS^* indicate that the activation complexes have more ordered structure than the reactants. The satisfactory values for the correlation coefficients from the Arrhenius plots of the thermal decomposition steps were observed to be $r \sim 1$ for all cases, which indicates a good fit with the linear function and reasonable agreement between the experimental data and the kinetic parameters.

Morphology analysis. Scanning electron microscopy (SEM) was employed to observe the morphology and particle size of the prepared complexes. The surface micrographs obtained with the SEM technique provide general information regarding the microstructure, surface morphology, particle size, chemical composition, and porous structures of the surfaces. The morphological phases of the formed CT complexes showed some uniform matrix in the SEM micrographs indicating the formation of a homogeneous material. Visible morphological change is observed between THM complexes. DNB complex shows a higher degree of homogeneity than the other complexes. The size of the particles differed substantially for each acceptors. Figures 8–10 show the SEM surface morphology of the synthesized THM complexes at different magnifications. The particles of

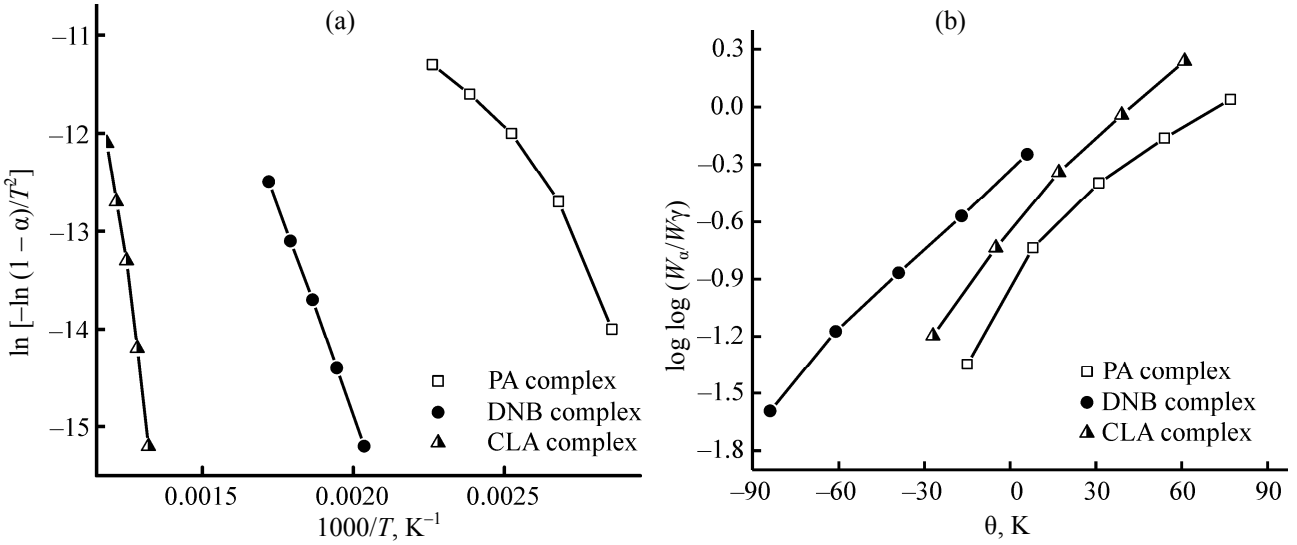

Fig. 7. Kinetic curves for THM complexes: (a) CR; Coats-Redfern equation and (b) HM; Horowitz-Metzger equation.

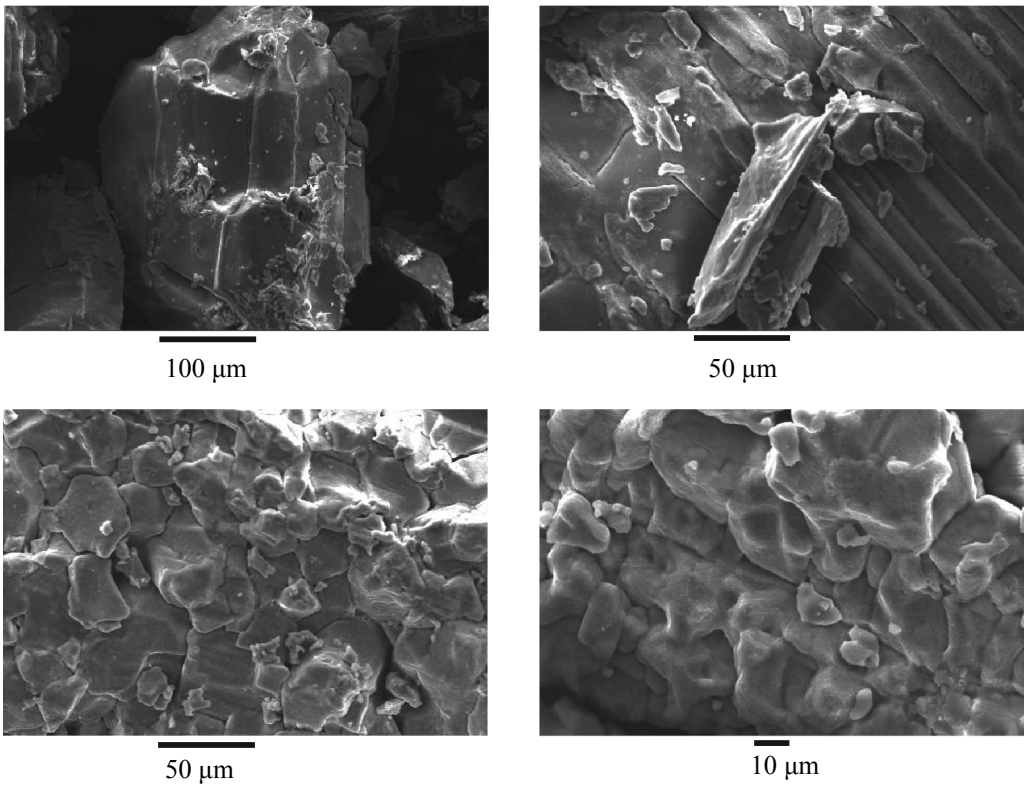

Fig. 8a. SEM micrographs of [(THM)(PA)] complex at different magnifications.

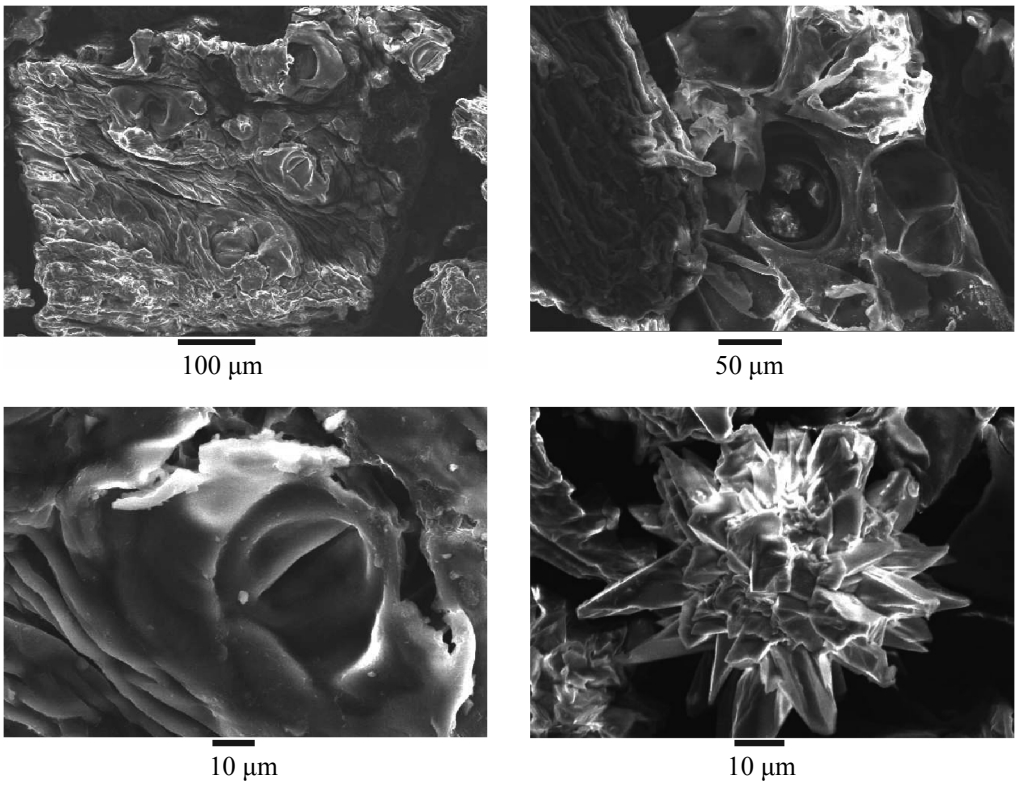

Fig. 9. SEM micrographs of [(THM)(CLA)] complex at different magnifications.

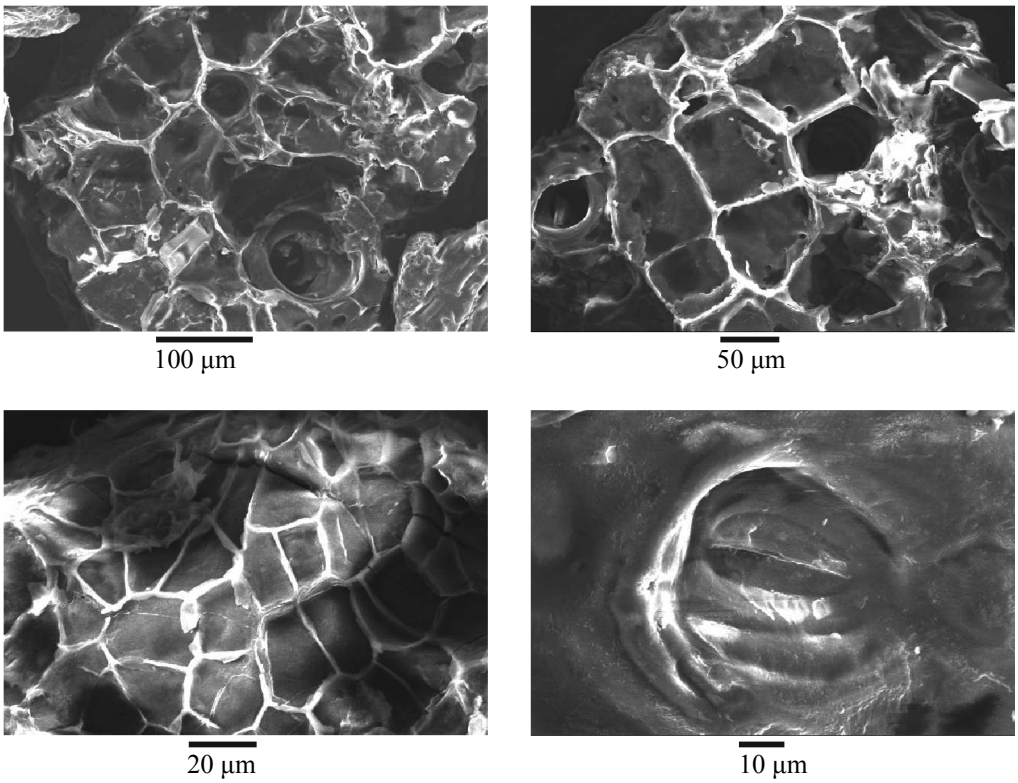

Fig. 10. SEM micrographs of [(THM)(DNB)] complex at different magnifications.

the PA complex appear as agglomerates and display a different granule size and shape with a particle size in the range of ~10–100 μm. A magnified SEM micrograph at a high magnification (×1000) of this complex (Fig. 8) show a densely packed granules with estimated particle size of ~10 μm. Figure 9 illustrates the surface morphology of the CLA complex. Their micrographs indicate that, this complex is semi-crystalline, as indicated by the formation of a single-phase with well-defended shape. This complex has clearly visible holes and a particle size in the range of ~10–100 μm. The DNB complex has a homogeneous matrix, as indicated by the uniformity and similarity of the particles. From the multi SEM micrographs with various degrees of enlargement (i.e., × 250, × 330, × 850, and × 1100) (Fig. 10), the particles of this complex have a cells-like structure. These particles exhibit different shapes with particle size in the range of ~10–100 μm. Comparing the morphology of THM complexes; one can see they are quite different in microstructure.

CONCLUSIONS

Recently, considerable attention has been devoted to the formation of stable CT complexes that result from the reaction between organic donors and acceptors. This interest stems from the significant physical and chemical properties of these complexes. The results reported in this paper are concerned with the structural, thermal and morphological studies of CT complexes formed between the THM as a donor and PA, CLA and DNB as a π-acceptor**.** The solid CT complexes were isolated and structurally characterized using elemental analysis, infrared (IR), Raman, ^{1}H NMR and thermogravimetric (TG) analysis. It is observed that the reaction stoichiometry is 1 : 1, and the resulting CT complexes were shown to have the general formula: [(THM)(acceptor)]. The interaction between the THM and the acceptors was taking please by the formation of intermolecular hydrogen bond. TG analysis indicates that the formation of complexes was thermally stable. The kinetic parameters (E^*, A, ΔS^*, ΔH^*, and ΔG^*) have been estimated. Their microstructure properties were also observed using SEM technique.

REFERENCES

1. Mulliken, R.S., *J. Am. Chem. Soc*., 1950, vol. 72, p. 4493.
2. Mulliken, R.S. and Pearson, W.B., *Molecular Complexes*, New York: Wiley Publishers, 1969.

3. Foster, R., *Charge Transfer Complexes*, London: Academic Press, 1969.
4. Mulliken, R.S., *J. Am. Chem. Soc*., 1952, vol. 74, p. 811.
5. Mulliken, R.S., *J. Phys. Chem*., 1952, vol. 56, p. 801.
6. Roy, T., Dutta, K., Nayek, M.K., Mukherjee, A.K., Banerjee, M., and Seal, B.K., *J. Chem. Soc., Perkin Trans. 2*, 1999, p. 2219.
7. Roy, D.K., Saha, A., and Mukherjee, A.K., *Spectrochim. Acta A*, 2005, vol. 61, p. 2017.
8. Slifkin, A.M., *Charge-Transfer Interaction of Biomolecules,* New York: Academic Press, 1971.
9. Dozal, A., Keyzer, H., Kim, H.K., and Wang, W.W., *Int. J. Antimicrob. Agent*, 2000, vol. 14, p. 261.
10. Korolkovas, A., *Essentials of Medical Chemistry*, 2nd ed., New York: Wiley, 1998, ch. 3.
11. Pandeeswaran, M., El-Mossalamy, E.H., and Elango, E.H., *Int. J. Chem. Kinet*., 2009, vol. 41, p. 787.
12. Pandeeswaran, M. and Elango, K.P., *Spectrochim. Acta A*, 2010, vol. 75, p. 1462.
13. Yakuphanoglu, F. and Arslan, M., *Solid State Commun*., 2004, vol. 132, p. 229.
14. Yakuphanoglu, F. and Arslan, M., *Opt. Mater*., 2004, vol. 27, p. 29.
15. Yakuphanoglu, F., Arslan, M., Kucukislamoglu, M., and Zengin, M., *Sol. Energy*, 2005, vol. 79, p. 96.
16. Andrade, S.M., Costa, S.M.B., and Pansu, R., *J. Colloid Interface Sci*., 2000, vol. 226, p. 260.
17. Jakubiak, R., Bao, Z., and Rothberg, L., *Synth. Met*., 2000, vol. 114, p. 61.
18. Eychmuller, A. and Rogach, A.L., *Pure Appl. Chem*., 2000, vol. 72, p. 179.
19. Das, S.K., Krishnamoorthy, G., and Dofra, S.K., *Can. J. Chem*., 2000, vol. 78, p. 191.
20. Smith, G., Bott, R.C., Rae, A.D., and Willis, A.C., *Aust. J. Chem*., 2000, vol. 53, p. 531.
21. Adam, A.M.A., Refat, M.S., and Saad, H.A., *J. Mol. Struct*., 2013, no. 1051, p. 144.
22. Adam, A.M.A., Refat, M.S., and Saad, H.A., *J. Mol. Struct*., 2013, no. 1037, p. 376.
23. Adam, A.M.A., *Spectrochim. Acta A*, 2013, no. 104, p. 1.
24. Khan, I.M. and Ahmad, A., *J. Mol. Struct*., 2013, no. 1050, p. 122.
25. Refat, M.S., Adam, A.M.A., Sharshar, T., Saad, H.A., and Eldaroti, H.H., *Spectrochim. Acta A,* 2014, no. 122, p. 34.
26. Refat, M.S., El-Sayed, M.Y., Adam, A.M.A., Saad, H.A., and Eldaroti, H.H., *Int. J. Electrochem. Sci*., 2013, no. 8, p. 4234.
27. Adam, A.M.A., Refat, M.S., Saad, H.A., and Eldaroti, H.H., *Eur. Chem. Bull*., 2012, no. 1(7), p. 241.
28. Kross, R.D. and Fassel, V.A., *J. Am. Chem. Soc*., 1957, vol. 79, p. 38.
29. Al-Attas, A.S., Habeeb, M.M., and Al-Raimi, D.S., *J. Mol. Struct*., 2000, no. 928, p. 158.
30. Coats, A.W. and Redfern, J.P., *Nature (London)*, 1964, no. 201, p. 68.
31. Horowitz, H.H. and Metzger, G., *Anal. Chem*., 1963, no. 35, p. 1464.